M. Bosund, A. Aierken, J. Tiilikainen, T. Hakkarainen, and H. Lipsanen. 2008. Passivation of GaAs surface by atomic-layer-deposited titanium nitride. Applied Surface Science, volume 254, number 17, pages 5385-5389.

Applied Surface Science 254 (2008) 5385–5389

Contents lists available at ScienceDirect

Applied Surface Science

journal homepage: www.elsevier.com/locate/apsusc

Passivation of GaAs surface by atomic-layer-deposited titanium nitride

M. Bosund *, A. Aierken, J. Tiilikainen, T. Hakkarainen, H. Lipsanen

Micro and Nanosciences Laboratory, Helsinki University of Technology, P.O. Box 3500, FI-02015 TKK, Finland

ARTICLE INFO

Article history:
Received 30 November 2007
Received in revised form 20 February 2008
Accepted 20 February 2008
Available online 26 February 2008

PACS:
81.15.Gh
78.55.Cr
78.55.-m
81.65.Rv
78.55.Qr

Keywords:
Atomic layer deposition
Gallium arsenide
Photoluminescence
Surface passivation
Titanium nitride

ABSTRACT

The suitability of titanium nitride (TiN) for GaAs surface passivation and protection is investigated. A 2–6-nm thick TiN passivation layer is deposited by atomic layer deposition (ALD) at 275 ° C on top of InGaAs/GaAs near surface quantum well (NSQW) structures to study the surface passivation. X-ray reflectivity measurements are used to determine the physical properties of the passivation layer. TiN passivation does not affect the surface morphology of the samples, but increases significantly the photoluminescence intensity and carrier lifetime of the NSQWs, and also provides long-term protection of the sample surface. This study shows that ALD TiN coating is a promising low-temperature method for ex situ GaAs surface passivation.

1. Introduction

Technology based on GaAs devices is not fully exploited partly because of the high density of interface and surface states that cause the surface Fermi level pinning near midgap of the forbidden band of bulk GaAs. The surface properties become increasingly important as the dimensions of the devices decrease. Therefore, surface passivation is one of the most important aspects when developing GaAs-based devices. A variety of different surface passivation techniques have been studied. Sulphur passivation methods have been developed but sulphur passivated GaAs surface suffers from a gradual degradation from air and light exposure [1]. Different plasma nitridation methods have faced problems with, e.g. formation of mixture of GaN and Ga_2O_3instead of pure GaN [2]. An ultrathin epitaxial GaN layer has also been used as a passivation layer [3]. However, the process temperature is more than 400 ° C which may be too high for many applications. Aluminum nitride (AlN) has been grown by using low temperature metalorganic vapour phase epitaxy (MOVPE) but the growth temperature is still above 370 ° C [4].

In this work GaAs surface passivation by ALD grown TiN is investigated. TiN deposition by ALD has been studied extensively in past [5]. This novel passivation technique has the following benefits compared to previously studied methods:

- Uniform growth at large area enables passivation of large amounts of components at the same time.
- Low process temperatures (275 °C), which can be important if passivation must be integrated as a part of component processing.
- Possibility to use as an ex situ passivation method.

Photoluminescence (PL) intensity and carrier lifetime of TiN coated InGaAs/GaAs NSQW structures are used to indicate the passivation efficiency. Passivation film properties like thickness, mass density and interface roughness are studied by X-ray reflectivity measurements. It is shown that TiN not only passivates but also protects the sample surface in the long run.

* Corresponding author. Tel.: +358 40 5178 665; fax: +358 94513128.
E-mail address: Markus.Bosund@tkk.fi (M. Bosund).

0169-4332/$ – see front matter © 2008 Elsevier B.V. All rights reserved.
doi:10.1016/j.apsusc.2008.02.070

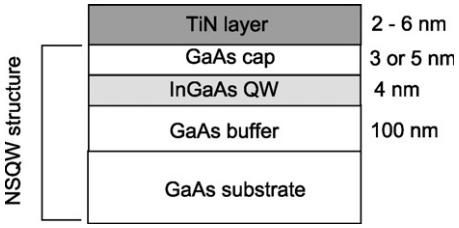

Fig. 1. Schematic diagram of a TiN passivated NSQW structure.

2. Experimental details

2.1. Samples

The schematic graph of a TiN passivated NSQW structure is shown in Fig. 1. A 4-nm-thick $In_{0.2}Ga_{0.8}As$/GaAs NSQW was grown on a semi-insulating GaAs (1 0 0) substrate in a horizontal MOVPE reactor at atmospheric pressure using hydrogen as the carrier gas. Tertiarybutylarsine (TMAs), trimethylgallium (TMGa) and trimethylindium (TMIn) were used as precursors for arsenic, gallium and indium, respectively. The NSQW was sandwiched by a 100 nm buffer and a top GaAs cap layer with thickness of 3 or 5 nm. The growth temperature was 650 °C. The V/III ratio for the $In_{0.2}Ga_{0.8}As$ was 23. The growth rate was 0.42 nm/s and 0.69 nm/s for GaAs and InGaAs, respectively. More details about MOVPE grown NSQWs has been reported elsewhere [6]. After MOVPE growth the NSQW sample was cleaved to several pieces, one was kept as a reference sample while the others were used for different ALD passivation processes. In this way we could avoid possible uniformity problems between different MOVPE growth runs.

Titanium nitride (TiN) was deposited by a flow type ALD apparatus (Beneq TFS 500) with continuous nitrogen carrier gas flow through the reactor. The pressure of the reactor during the growth was about 3.2 mbar. Titanium tetrachloride ($TiCl_4$) and ammonia (NH_3) were used as precursors. Trimethylaluminum ($(CH_3)_3Al$, TMA) was used as a reducing agent between $TiCl_4$and NH_3 pulses. TMA improves the film quality and makes it possible to use lower growth temperature. $TiCl_4$ pulse length was 400 ms and purge time 7 s. TMA pulse length was 200 ms and purge time 2 s. NH_3 pulse time was 300 ms and purge time 7 s. The growth temperature was 275 ° C and the liquid precursors ($TiCl_4$ and TMA) were kept at 20 °C. The vapor pressures for the $TiCl_4$ and TMA at 20 ° C were 11.4 and 9.8 mbar, respectively. Ammonia tank was at room temperature.

2.2. Measurements

TiN film properties like thickness, mass density and surface roughness were studied by using X-ray reflectivity (XRR) measurements. Philips X'pert Pro instrument was used at 40 kV voltage and 40 mA current settings. The measurement assembly consisted of Ni and Cu attenuators (Cu attenuator factor 180), a X-ray mirror, a Soller slit (0.04 rad) and a programmable divergence slit at 1/32° fixed aperture and a 10 mm X-ray mask at incident beam setup. The reflected beam was collected by using a thin film collimator, a 0.04 radian Soller slit, a flat graphite crystal monochromator and a scintillation detector assembly.

The low temperature (10 K) continuous-wave photoluminescence (PL) measurements were made by using a diode-pumped frequency doubled Nd:YVO_4 laser emitting at 532 nm wavelength for excitation. A monochromator, a liquid-nitrogen-cooled germanium detector and a lock-in amplifier were used to record the PL spectra. The low temperature time-resolved photoluminescence (TRPL) measurements were performed by exciting the samples with 150 fs pulses at 780 nm from a mode locked Ti:Sapphire laser and by detecting the signal using a Peltier-cooled microchannel plate multiplier and time-correlated single photon counting electronics.

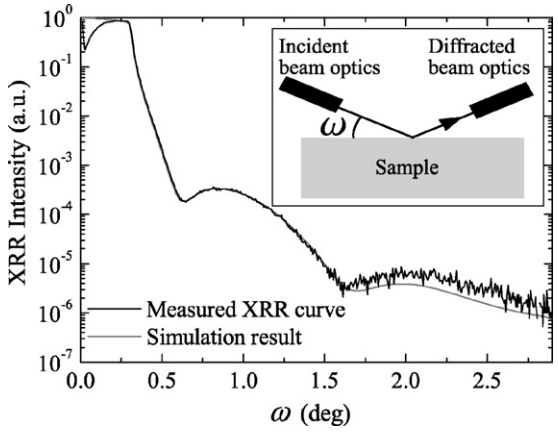

Fig. 2. Measured and simulated XRR curves of a 60 cycles TiN layer on GaAs (1 0 0) substrate. The schematic picture of the measurement setup is shown in the inset.

Contact mode atomic force microscopy was used to study the surface morphology of the samples.

3. Results and discussion

3.1. Physical propetries of ALD grown TiN

The linearity of the TiN growth (at 275 °C) on GaAs (1 0 0) substrate was studied by changing the number of ALD growth cycles. Fig. 2 shows the measured and simulated XRR curves of a 60 cycles TiN layer. The simulated curve is based on Parrat's formalism [7] and the Nevot–Croce roughness model [8]. The physical model differs from the real measurement because the sample area is not infinite and X-ray thickness is not zero. That effect is largest when the angle ω is less than 0.2°. However, the most interesting point in this study is the layer thickness which is related to the XRR curve fringe spacing. The dependence of the TiN layer thickness on the number of ALD growth cycles is shown in Fig. 3. TiN layer thickness is linearly increasing when the number of the growth cycles is more than 20. The intercept of the fitted line with the thickness-axis is 1.1 nm which is typically a consequence of substrate native oxide formation before growth or so called

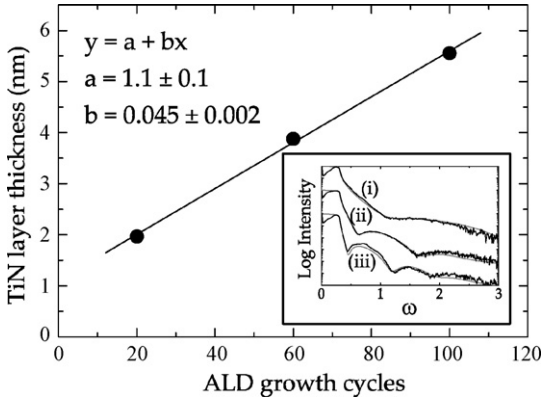

Fig. 3. TiN layer thickness on GaAs substrate as a function of growth cycles based on the XRR measurements. A linear fitting formula is represented so that y is layer thickness, x is number of cycles and a and b are linear fitting parameters in nanometer scale. The inset shows measured (black) and simulated (gray) curves for (i) 20 cycles, (ii) 60 cycles and (iii) 100 cycles of TiN on GaAs.

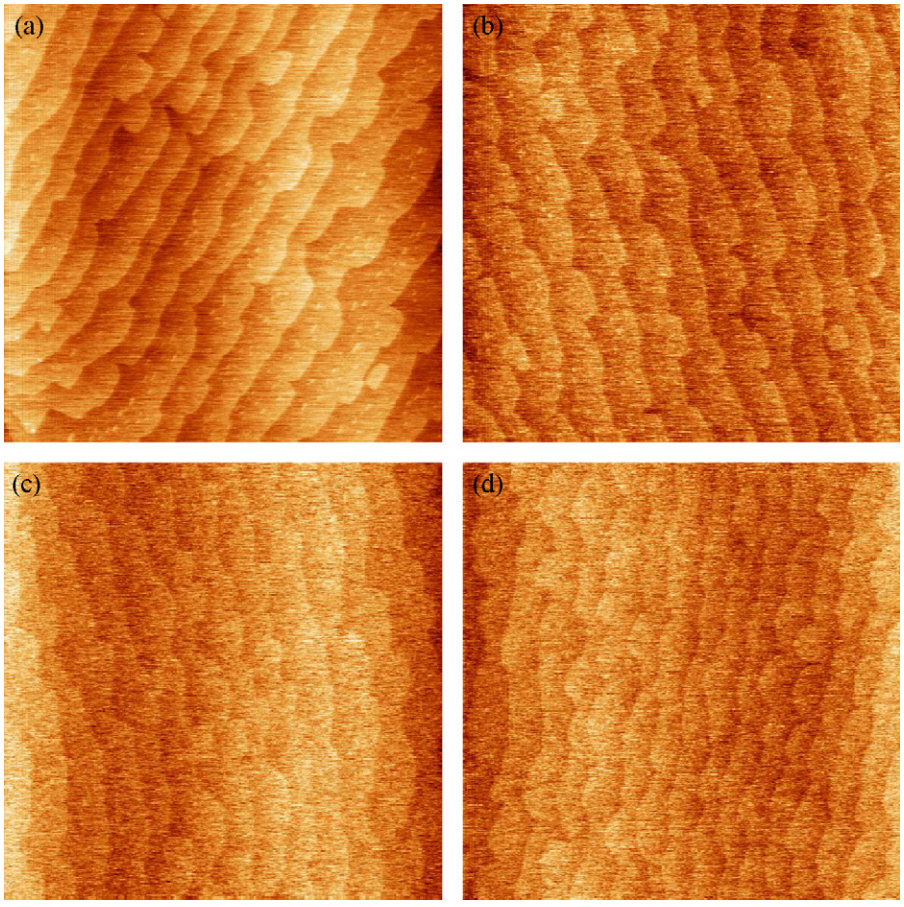

Fig. 4. AFM surface images of (a) unpassivated and (b–d) TiN passivated NSQW samples. The thickness of the TiN layer is (b) 2.9 nm, (c) 3.9 nm and (d) 5.6 nm. Image size is 5 μm ×5 μm and vertical scale is 3 nm.

surface enhanced growth [9]. In this study native oxide was removed by using hydrofluoric acid etching before ALD growth. Thus it can be assumed that the grown layer consists mostly of titanium nitride and no significant oxidation occurs at the GaAs/TiN interface. The slope of the fitted line gives the growth rate, which is in this case approximately 0.05 nm/cycle. The growth rate was confirmed by spectroscopic ellipsometer measurements of a thick (2000 cycles) TiN layer grown on silicon. The physical parameters obtained from the XRR measurements are given in Table 1. The mass density of the TiN layer decreases slightly when the layer thickness is increased.

When a thin film is grown onto substrate, biaxial strain may appear in the substrate material near the boundary. To investigate whether the TiN layer causes strain to the GaAs substrate, high resolution X-ray diffraction (XRD) measurements were carried out. Variation of the TiN layer thickness from 0 to 6 nm did not affect the shape of the rocking curves taken around the GaAs (004) diffraction peak, i.e., TiN thin films do not cause strain to the substrate. In order to investigate the TiN film crystallinity a thick (about 100 nm) TiN layer was grown on a HF etched Si substrate for XRD powder measurement. In this study no XRD peaks were observed which indicates that TiN growth at 275 ° C yields amorphous films.

Table 1
Physical parameters of ALD grown TiN layers on GaAs (1 0 0) substrate based on the XRR measurements

Growth cycles	Thickness (nm)	Density (g/cm^3)	Roughness (nm)
20	2.0	3.4	0.4
60	3.9	3.3	0.8
100	5.6	3.2	0.7

The resistivity of TiN was measured by the transmission line method to be 1.6 m Ωcm. The crystalline bulk TiN has a much smaller resistivity of 21.7×10^{-3} m Ω cm [12]. This difference is a consequence of chlorine impurities which increase the resistivity [5].

3.2. GaAs surface passivation by ALD grown TiN

The passivation effect was studied by changing the thickness of the TiN layer and measuring the surface morphology, PL intensity and TRPL transients of the NSQWs. A series of samples was made by changing the TiN layer thickness from 2.0 to 5.6 nm. The optical measurements were also carried out after 1-month air exposure to bring out the time dependence of the passivation effect.

Fig. 4 shows the AFM images of the unpassivated and TiN passivated NSQW samples. Smooth sample surfaces are observed but the atomic layer terraces are less clear for the passivated samples because of the amorphous TiN film. However, the passivation layers do not significantly affect the surface morphology of the samples.

Low temperature PL curves for an unpassivated reference sample and a TiN passivated NSQW are shown in Fig. 5. Difference in PL intensities between the two samples clearly indicates the efficiency of the TiN passivation. The TiN layer also protects the sample surface against long-term oxidation since the PL intensity difference is even more pronounced after 1-month air exposure.

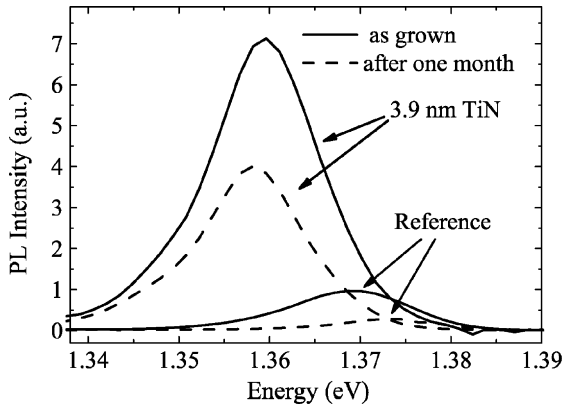

Fig. 5. Low temperature PL curves for an unpassivated reference and a TiN passivated (3.9 nm TiN layer) NSQW before and after 1-month air exposure.

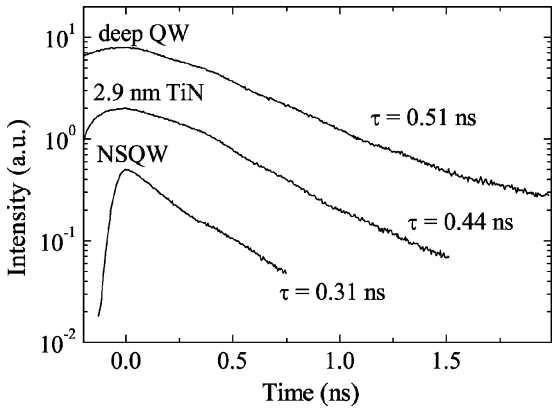

Fig. 7. Low-temperature TRPL transients (series B after 1 month) of an unpassivated NSQW, a TiN passivated NSQW, and a deep QW. Curves are normalized and vertically shifted for clarity.

The redshift of the PL peak is probably caused by random fluctuation of the indium composition of the QW. We point out that although the PL peak position was slightly changing quite randomly between the samples the PL intensity of the samples was not changing randomly.

The maximum PL intensity of the TiN passivated InGaAs NSQWs is shown in Fig. 6 as a function of the passivation layer thickness. In series A and B the thickness of the GaAs cap is 5 and 3 nm, respectively. Both series show similar behavior; the maximum PL intensity is obtained when the TiN layer is about 4-nm thick (60 cycles). It can be seen that the PL intensity is up to 15 times higher compared to the unpassivated (zero cycles) reference. When the thickness is increased to 5.6 nm (100 cycles) the PL intensity drops substantially. The reason for this behavior is discussed later in this paper. Series B shows weakened PL intensities after 1-month air exposure, especially for the thin layers (0–3 nm). Oxygen can diffuse easier through thin layers and oxidize the GaAs/TiN interface which increases the number of surface states.

If the passivation method eliminates the possibility of the surface recombinations completely the thickness of the GaAs cap layer does not affect the PL intensity of the NSQW. However, the relative PL intensity is higher in the series A compared to B. Therefore it can be assumed that the surface recombinations in the GaAs/TiN boundary decrease the PL intensity of the NSQW when the cap layer is thin. In the light of these results, the TiN layer reduces the number of GaAs surface states but does not eliminate them completely. This result is in agreement with the TRPL results presented later in this paper.

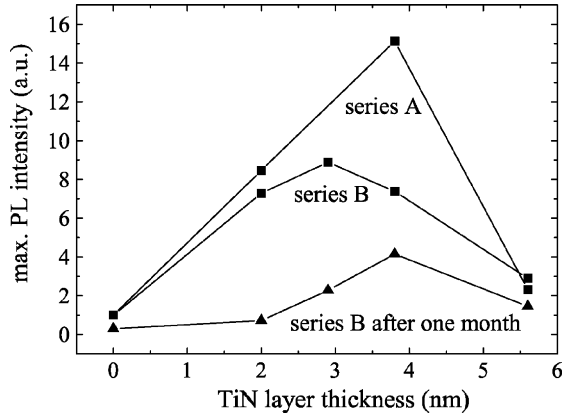

Fig. 6. Maximum PL intensity of TiN coated NSQWs as a function of the TiN layer thickness. The thickness of the GaAs cap is 5 nm in series A and 3 nm in series B. The PL intensity of the reference samples in series A and B are normalized to one.

A similar MOVPE passivation technique for InGaAs NSQWs has been studied by growing e.g. a few monolayers of indium phosphide (InP) or gallium nitride onto a NSQW structure [3,10]. These treatments improved the PL intensity of the NSQW several order of magnitudes. One reason for the clearly better passivation results with MOVPE is that the passivation was made directly after the NSQW growth *in situ*. In that case there is no possibility for the oxidation of the GaAs surface before the passivation layer is grown. One significant difference in ALD TiN passivation compared to the MOVPE is the thickness of the passivation layer. The ALD TiN layer thickness was in the nanometer scale in this study whereas the layers in the MOVPE based passivation studies [3,10] were from one to three monolayers thick. The ultrathin layers were used because of lattice mismatch problems with thicker layers.

The extent of several different sulphur solutions as a GaAs passivation method has been studied in reference [11] by using the PL intensity of GaAs to indicate the passivation efficiency. It was shown that the PL intensity of the sulphur passivated GaAs decreased rapidly during the first 5 h. After 1 month the PL intensity of the samples was less than four times higher compared to an unpassivated reference (after 1 month). Compared to that result the ALD TiN passivation method presented in this paper is more stabile. It can be seen from Fig. 5 that the PL intensity of the ALD passivated NSQW (with the 5.6 nm TiN layer) was 15 times higher compared to the unpassivated reference NSQW after 1-month air exposure.

The low-temperature TRPL transients of an unpassivated reference, a TiN passivated NSQW, and a deep QW (similar QW but the thickness of the GaAs cap is 20 nm) taken at the wavelength of the maximum continuous-wave PL intensity are shown in Fig. 7. The decay time τ was determined from the transients by using the first-order exponential fit $I(t) = A\exp(-t/\tau)$. The measured carrier

Table 2
Carrier lifetime parameters of TiN passivated NSQWs

Sample	τ (ns)	$\Delta\tau$ (ns)	τ_{NR} (ns)
Unpassivated	0.31	±0.02	0.79
Deep QW	0.51	±0.02	–
2.0 nm TiN passivated	0.44	±0.02	3.2
2.9 nm TiN passivated	0.44	±0.02	3.2
3.9 nm TiN passivated	0.42	±0.02	2.4
5.6 nm TiN passivated	0.43	±0.02	2.7

The measured lifetime τ is determined from the TRPL transients (series B measured after 1-month air exposure) and the nonradiative lifetime τ_{NR} is calculated by using the Eq. (1). The error ($\Delta\tau$) of the measured lifetime is estimated by fitting trial curves to the TRPL transient data.

lifetime (decay time) of a NSQW can be expressed as [13,14]

$$\frac{1}{\tau} = \frac{1}{\tau_R} + \frac{1}{\tau_{NR}} \quad (1)$$

where τ_R is the lifetime for radiative carrier recombination in a QW with an infinitely thick cap layer and τ_{NR} is the lifetime for nonradiative recombination by surface states. The deep QW gives the highest decay time of 0.51 ns. We consider the deep QW as a QW with an infinitely thick cap layer and thus assume that the measured decay time in that case is the same as a radiative lifetime. In other words $\tau = \tau_R$ for deep QW. Since in this study all the QWs have a similar structure, we further assume that τ_R is same for all the NSQWs. The nonradiative lifetime τ_{NR} can then be calculated using the Eq. (1).

The measured (after 1-month air exposure) decay times and calculated nonradiative lifetimes are listed in Table 2. The decay time is increased significantly by TiN passivation. The nonradiative lifetimes of the TiN coated samples are three to four times larger compared to the unpassivated sample. This is in good agreement with the observed enhancement of the PL intensity and thus further indicates the passivation efficiency.

Unlike the PL intensity, the decay time (and thus the nonradiative lifetime) does not change significantly when the TiN thickness is increased from 4 to 6 nm. This suggests that the passivation efficiency is actually quite independent of the TiN layer thickness. In case of the 5.6 nm TiN layer only about 11% of light is absorbed (the absorption coefficient of TiN was determined to be about 2×10^5 cm^{-1} in the near infrared region by spectroscopic ellipsometer measurements), which is too small to explain the observed reduction of PL intensity (Fig. 6). Also no strain were observed in XRD measurements. We assume that when the thickness of the TiN layer is increased from 4 to 6 nm the reflectivity in the GaAs/TiN and air/TiN interfaces changes and the reduced PL intensity is then a consequence of decreased light transmission.

4. Conclusions

In summary, the surface passivation of near-surface InGaAs QWs by ALD grown TiN thin films was investigated. TiN growth was linear with a growth rate of 0.05 nm/cycle when the number of cycles was more than 20. The surface morphology of the samples was not significantly affected by the amorphous TiN films. The low-temperature PL and TRPL measurements showed that the TiN passivation increases significantly the PL intensity and carrier lifetime of the NSQWs. Although the PL intensity decreased when the TiN layer was thicker than 4 nm, the TRPL results indicated that the passivation efficiency was quite independent of the TiN film thickness. The TiN layer also protected the sample surface against oxidation in the long run. The results suggest that atomic layer deposited TiN is a promising low-temperature ex situ passivation material.

Acknowledgements

The authors acknowledge the Finnish Agency for Technology and Innovation (TEKES, ALDUS Project) and Academy of Finland for supporting this work financially.

References

[1] K. Sato, H. Ikoma, Jpn. J. Apl. Phys., Part 1 32 (1993) 921.
[2] S. Anantathanasarn, S. Ootomo, T. Hashizume, H. Hasegawa, App. Surf. Sci. 159/160 (2000) 456–461.
[3] J. Riikonen, J. Sormunen, H. Koskenvaara, M. Mattila, M. Sopanen, H. Lipsanen, J. Cryst. Growth 272 (2004) 621–626.
[4] S. Fujieda, M. Mizuta, Y. Matsumoto, Adv. Mater. Optics Electron. 6 (1996) 127–134.
[5] M. Juppo, P. Alen, M. Ritala, M. Leskelä, Chem. Vap. Depos. 7 (5) (2001) 211–217.
[6] H. Lipsanen, M. Sopanen, M. Taskinen, J. Tulkki, J. Ahopelto, Appl. Phys. Lett 68 (16) (1996).
[7] L.G. Parratt, Phys. Rev. 95 (2) (1954) 359–369.
[8] L. Nevot, P. Croce, Rev. de Phys. Appl. 15 (2) (1980) 761–780.
[9] R. Puurunen, W. Vandervorst, J. Appl. Phys. 96 (2004) 7686–7695.
[10] A. Aierken, J. Riikonen, J. Sormunen, M. Sopanen, H. Lipsanen, Appl. Phys. Lett. 88 (2006) 221112-1–2211123-2211123.
[11] Y. Wang, Y. Darici, P.H. Holloway, J. Appl. Phys. 71 (1992) 2746–2754.
[12] K. Yokota, K. Nakamura, T. Kasuya, K. Mukai, M. Ohnishi, J. Phys. D: Appl. Phys. 37 (2004) 1095–1101.
[13] W. Shockley, Electrons and Holes in Semiconductors, van Nostrand, New York, 1950, p. 318.
[14] J. Dreybrodt, F. Daiminger, J.P. Reithmaier, A. Forchel, Phys. Rev. B 51 (7) (1995) 4657–4660.